

Recognizing factors affecting decline in groundwater level using wavelet-entropy measure (case study: Silakhor plain aquifer)

Mehdi Komasi and Soroush Sharghi

ABSTRACT

The most important approach to identify the behavior of hydrological processes is time series analysis of this process. Wavelet-entropy measure has been considered as a criterion for the degree of time series fluctuations and consequently uncertainty. Wavelet-entropy measure reduction indicates the reduction in natural time series fluctuations and thus, the occurrence of an unfavorable trend in time series. In this way, to identify the main cause of declining aquifer water level in the Silakhor plain, monthly time series of rainfall, temperature and output discharge were divided into three different time periods. Then, these time series were decomposed to multiple frequent time series by wavelet transform and then, the wavelet energies were computed for these decomposed time series. Finally, wavelet-entropy measure was computed for each different time period. Given the entropy reduction of about 71, 13 and 10.5% for discharge, rainfall and temperature time series respectively, it can be concluded that fluctuation decrease of discharge time series has relatively more effect on groundwater level oscillation patterns with respect to the rainfall and temperature time series. In this regard, it could be concluded that the climate change factors are not facing significant changes; thus, human activities can be regarded as the main reason for the declining groundwater level in this plain.

Key words | climate change impacts, complexity decrease, groundwater level, human activities, Silakhor plain, wavelet-entropy measure

Mehdi Komasi (corresponding author)
Faculty of Civil Engineering,
Ayatollah Boroujerdi University,
Boroujerd,
Iran
E-mail: komasi@abru.ac.ir

Soroush Sharghi
Water Engineering and Hydraulic Structures,
Ayatollah Boroujerdi University,
Boroujerd,
Iran

INTRODUCTION

Water resources management can help to ensure the sustainable use of water resources such as groundwater for urban and rural water supply. Decline in groundwater levels not only limits groundwater exploitation but also causes land subsidence and human-financial losses.

Several studies noted the significant relationship between climate change and the decline in groundwater level (Zwolsman & van Bokhoven 2007; Waibel *et al.* 2013; Chinnasamy & Ganapathy 2018). Hao *et al.* (2008) investigated that climate change has resulted in increasing global atmospheric temperatures and a modified rainfall pattern,

which may have a direct impact on groundwater levels. It has been shown that groundwater systems have undergone changes due to human activities including groundwater abstraction, recharge and reservoir construction (Xue *et al.* 2014; Singh *et al.* 2016; Yang *et al.* 2017; Amaranto *et al.* 2018; Deng *et al.* 2018).

Generally, discussions related to drought and water crisis have been in conflict with each other and achieve no consensus and a comprehensive and clear purpose as yet. Several researchers have argued that the water crisis is the result of extensive climate change (Rabbani & Alikhani

2010; Vahidi 2011), and several studies have considered the indiscriminate use and lack of proper management of water resources as the main factors of drought and water crisis (Fakhodi & Mirzaie 2013; Nourani *et al.* 2015a, 2015b; Varouchakis *et al.* 2016).

Undoubtedly, studies on water level fluctuations (or groundwater level fluctuations) are important for water resources deterioration and testing the impacts of the natural climate fluctuation or human-induced climate changes on hydrology, and also in modeling water levels to use those for quantitative interpretation (Cimen & Kisi 2009; Kakahaji *et al.* 2013). Furthermore, various studies have been carried out in modeling and statistical analysis of water level fluctuations in different watersheds over the world (Kebede *et al.* 2006; Cimen & Kisi 2009; Kakahaji *et al.* 2013).

In recent years, the groundwater level of Silakhor plain in Iran has been substantially reduced. The fluctuating pattern of groundwater level time series of this plain has changed. Changes in time series fluctuations may be considered as the occurrence of an unfavorable trend. So, it is essential to determine the causes of these changes in groundwater level. To demonstrate the impact of climate change, temperature and rainfall time series are investigated and to monitor the impacts of human activities such as digging illegal wells, and the unprecedented increase in agriculture and industrial plants, the output discharge time series of the basin is used. In this way, various indices including the new wavelet-entropy measure can be used to rank the impact of each factor.

For the first time, Shannon (1948) introduced the concept of entropy as a tool to measure the information content of the signal. Many researchers have investigated the concept of Shannon entropy in order to analyze signals (Bercher & Vignat 2000; Shardt & Huang 2013; Chen & Li 2014; Castillo *et al.* 2015; Singh & Cui 2015; Varanis & Pederiva 2015). Pincus (1991) demonstrated a model from the concept of entropy, named approximate entropy, in order to determine the complexity of short-term time series. Richman & Moorman (2000) published a paper in which they defined the sample entropy, which is a modification of approximate entropy. Costa *et al.* (2002) defined and applied multi-scale entropy, which is based on sample entropy and is effective in analyzing the complexity of

physiological signals. They pointed out that multi-scale entropy robustly separates healthy and pathologic groups and consistently yields higher values for simulated long-range correlated noise compared to uncorrelated noise. Mishra *et al.* (2009) applied the concept of entropy to investigate the spatial and temporal variability of rainfall time series for the state of Texas, USA. In their study, marginal entropy was employed to clarify the variability associated with monthly, seasonal, and annual time series. Ming Chou (2011) studied the application of multi-scale entropy for analyzing complex rainfall time series and finding the number of resolution levels in the wavelet decomposition. Their analysis revealed that the suggested number of resolution levels can be obtained using multi-scale entropy analysis. Meanwhile Shannon entropy is the most commonly and effectively used entropy. The conjunction of entropy and wavelet concepts has been used to develop a new complexity measure of wavelet-entropy (Rosso *et al.* 2006).

In addition to the aforementioned studies, it should be noted that in past decades several methods have been proposed to measure the complexity and consequently time series change detection and modeling. For example, Fathian *et al.* (2016) used Seasonal Auto Regressive Integrated Moving Average (SARIMA) in order to study Urmia Lake's water level change. This article aims to identify the changes in the statistical characteristics in terms of trend, stationarity, linearity/nonlinearity and change point detection analyses. Meanwhile, based on research by Fathian *et al.* (2016), the SARIMA model effectively detects and interprets fluctuations in time series when composed by other models such as Generalized Autoregressive Conditional Heteroscedasticity (GARCH). This apparently is an appropriate method but depends on too much computational effort and highly precise determination of the SARIMA input parameters.

Eliciting beneficial information from hydrological time series and structural characteristics of annual precipitation in Lake Urmia Basin, Vaheddoost & Aksoy (2017) calculate entropy in each proposed station with respect to the long-run mean precipitation of the basin. Several tests for consistency, randomness, trend and best-fit probability distribution function are applied to investigate characteristics of the annual precipitation. Due to the north-south oriented mountains, a relatively sharp decline in precipitation from

west to east can be compared to the gradual decline in precipitation from north-south due to the smooth change in terrain. The aforementioned study aimed at identifying the structural characteristics of annual precipitation but it did not sufficiently address the effect of other hydrological time series on annual precipitation. Given that the uncertainty changes in a hydrological time series can influence the other time series, it is extremely crucial to survey the mutual interdependency of a couple of time series with regard to an uncertainty analysis method such as wavelet-entropy.

According to the mentioned works, it can be concluded that the wavelet-entropy measure is a new and efficient index to determine the complexity of time series, especially hydrological time series. Therefore, the intention of the present study is to investigate the impact of temperature, rainfall and output discharge changes on the decline in the groundwater level of Silakhor plain aquifer using the wavelet-entropy measure. Since the time series of the hydrological processes are very complicated, using wavelet transform and decomposing time series into its sub-signals can lead to an accurate understanding of short- and long-term behavior of the time series (Nourani *et al.* 2012). Wavelet transform provides useful decompositions of main time series so that wavelet-transformed data can improve the ability to analyze time series by capturing useful information on various resolution levels (Rajaei *et al.* 2010; Nourani *et al.* 2012; Komasi & Sharghi 2016).

The other sections of this paper are organized as follows. In the next section, the concepts of wavelet

transform and wavelet-entropy measure are briefly reviewed, and then the study area is introduced. Human activities and climate change impacts in the study basin are discussed and investigated using wavelet-entropy measure in the following section. Concluding remarks are presented in the final section of the paper.

METHODS

Wavelet transform

The wavelet transform has increased in usage and popularity in recent years since its inception in the early 1980s, yet it still does not enjoy the widespread usage of the Fourier transform. Fourier analysis has a serious drawback. In transforming to the frequency domain, time information is lost. When looking at a Fourier transform of a signal, it is impossible to tell when a particular event took place but wavelet analysis allows the use of long time intervals where we want more precise low-frequency information, and shorter regions where we want high-frequency information. Figure 1 compares Fourier transform and wavelet transform.

In the field of earth sciences, Goupillaud *et al.* (1984), who worked especially on geophysical seismic signals, introduced the wavelet transform application. A comprehensive literature survey of wavelet in geosciences can be found in Labat (2005). As there are many good books and articles

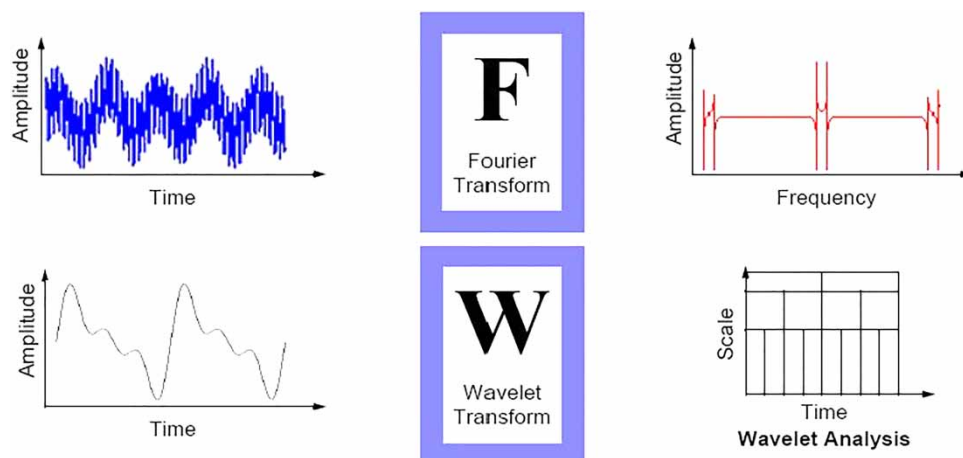


Figure 1 | Comparison of Fourier and wavelet transforms.

introducing the wavelet transform, this paper will not delve into the theory behind wavelets and only the main concepts of the transform are briefly presented; recommended literature for the wavelet novice includes Mallat (1998). The time-scale wavelet transform of a continuous time signal, $x(t)$, is defined as (Mallat 1998):

$$T(a, b) = \frac{1}{\sqrt{a}} \int_{-\infty}^{+\infty} g^* \left(\frac{t-b}{a} \right) x(t) \cdot dt \quad (1)$$

where $*$ corresponds to the complex conjugate and $g(t)$ is the wavelet function or mother wavelet. The parameter a acts as a dilation factor, while b corresponds to a temporal translation of the function $g(t)$, which allows the study of the signal around b . The main property of wavelet transform is to provide a time-scale localization of processes, which derives from the compact support of its basic function. This is opposed to the classical trigonometric function of Fourier analysis. The wavelet transform searches for correlations between the signal and wavelet function. This calculation is carried out at different scales of a and locally around the time of b . The result is a wavelet coefficient ($T(a,b)$) contour map known as a scalogram. So the original signal may be reconstructed using the inverse wavelet transform as:

$$x(t) = \frac{1}{c_g} \int_{-\infty}^{+\infty} \int_0^{\infty} \frac{1}{\sqrt{a^g}} \left(\frac{t-b}{a} \right) T(a, b) \frac{da \cdot db}{a^2} \quad (2)$$

For practical applications, the hydrologist does not have at his or her disposal a continuous-time signal process but rather a discrete-time signal. A discretization of Equation (2) based on the trapezoidal rule may be the simplest discretization of the continuous wavelet transform. This transform produces N^2 coefficients from a data set of length N ; hence redundant information is locked up within the coefficients, which may or may not be a desirable property. To overcome the mentioned redundancy, logarithmic uniform spacing can be used for the a scale discretization with correspondingly coarser resolution of the b locations, which allows for N transform coefficients to completely describe a signal of length N . Such a discrete wavelet has the form

(Mallat 1998):

$$g_{m,n}(t) = \frac{1}{\sqrt{a_0^m}} g \left(\frac{t - nb_0 a_0^n}{a_0^m} \right) \quad (3)$$

where m and n are integers that control the wavelet dilation and translation respectively; a_0 is a specified fixed dilation step greater than 1; and b_0 is the location parameter and must be greater than zero. The most common and simplest choice for parameters are $a_0 = 2$ and $b_0 = 1$. This power-of-two logarithmic scaling of the translation and dilation is known as the dyadic grid arrangement.

Wavelet-entropy measure

As a complexity criterion, in this paper, wavelet-entropy is used to measure complexity, which is able to handle different time scales at different resolutions in time series with different spatiotemporal characteristics as a multi-scale analysis. For computing wavelet-entropy, time series are decomposed in the same level using wavelet transform; then, wavelet-entropy and related energies in each level are obtained. Finally, the multi-scale entropy is measured. The energy at each resolution level as $m = 1, 2, 3, \dots, M$, will be the energy of the detailed signal (Rosso *et al.* 2006):

$$E_m = \|r_m\|^2 = \sum_n |C_m(n)|^2 \quad (4)$$

where C_m and n are current partial coefficients and the number of current coefficients in scale m , respectively and the total energy will be (Rosso *et al.* 2006):

$$E_{total} = \sum_m \sum_n |C_m(n)|^2 = \sum_m E_m \quad (5)$$

Wavelet energy can be normalized as below which represents the relative wavelet energy (Rosso *et al.* 2006):

$$\rho_m = \frac{E_m}{E_{total}} \quad (6)$$

Entropy has been considered as a criterion of the degree of uncertainty, tranquility and redundancy. Ranging from zero to one, the greater value of ρ_m indicates the high

degree of fluctuation of a variable (so-called uncertainty) and vice versa. It is noteworthy to mention that the physical meaning of different values of entropy measure is interpreted as follows: when the occurrence probability (historical frequency) of a phenomenon in a special period is low, the uncertainty of the aforementioned phenomenon

is high, resulting in extreme fluctuation of the time series. On the other hand, the higher the entropy value of a time series is, the higher influence of the time series value to other related time series has. This concept can be derived from Equation (7).

In static signals, it is possible to use the entropy concept for measuring the relative complexity. If the entropy of time series is high and contains more random values and more irregularity, they will have higher complexity. Entropy has been used to define the wavelet-entropy (Rosso *et al.* 2001).

$$WE = - \sum_m \rho_m \cdot Ln[\rho_m] \tag{7}$$

where ρ_m is defined in Equation (6). Thus, the wavelet-entropy is considered as an indicator to measure the degree of signal complexity and uncertainty of a phenomenon (Rosso & Mairal 2001). Figure 2 presents the flow chart to calculate the wavelet-entropy measure schematically. As shown in Figure 2, time series are decomposed into sub-signals with various resolution levels by wavelet transform; then, the normalized energy of each sub-signal is calculated. Finally, wavelet-entropy measure is obtained with respect to the normalized energies using Equation (7). It is notable that there are different irregular mother wavelets such as Haar, db2, sym3 and coif1 (Komasi & Sharghi 2016) which are shown in Figure 3. In this study, db2 mother wavelet is applied due to its resemblance to

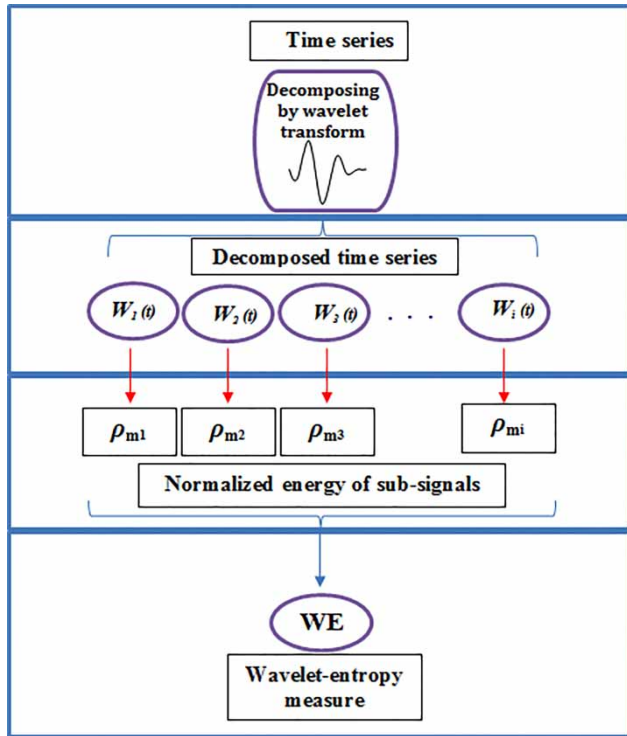


Figure 2 | Schematic structure of calculating wavelet-entropy measure.

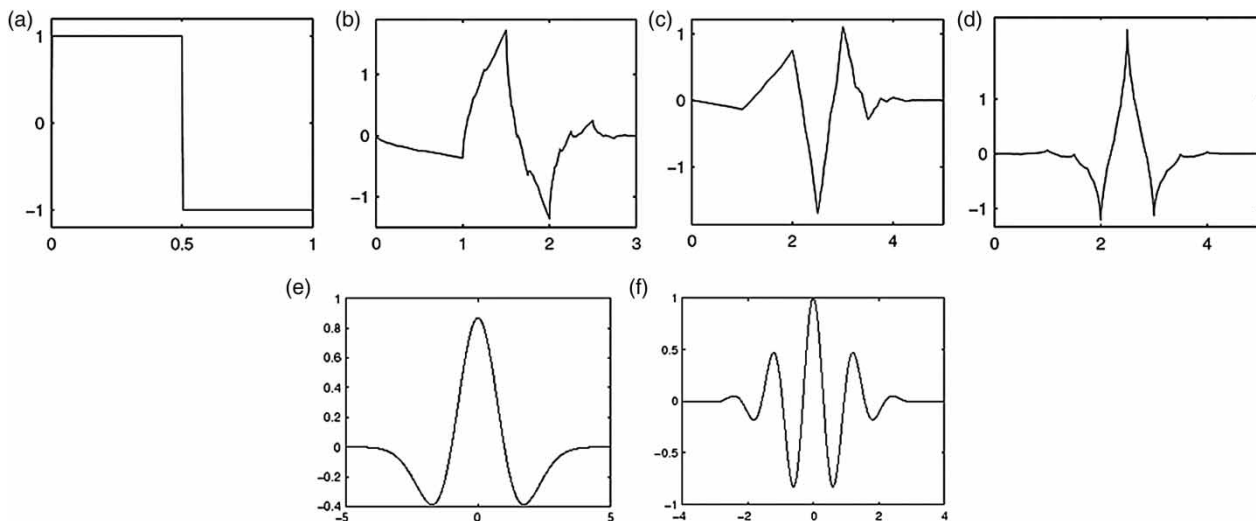


Figure 3 | (a) Haar, (b) Db2, (c) Sym3, (d) Coif1, (e) Mexican hat, (f) Morlet.

the signal fluctuations of the hydrological process, particularly the groundwater level fluctuations. Further details about the physical understanding of mother wavelet functions are provided in Komasi & Sharghi (2016).

CASE STUDY

Silakhor plain is the largest flat land in Lorestan province, Iran, covering an area of 819 km² (Figure 4). It is located in the northeast of Lorestan consisting most of the populated parts of Borujerd, Dorud and Azna counties. Silakhor plain is a grassland plain expanding from northwest to southeast along the elevated reliefs of Zagros Mountains. It is an upper section of Karun River's basin and its elevation varies between 1,437 and 3,845 m above sea level. Silakhor plain plays a key role in agriculture and horticulture. The Silakhor plain is composed of two main substances: lime and transformed-igneous. The main formations of the region in its west and northwest are lime and carbonate formation with many cracks and slits, while on the eastern and southeastern of this aquifer, more granite and gneiss and transformed, igneous formation could be found. The dominant land use in Silakhor plain is agriculture.

The statistical characteristics of Silakhor plain are categorized in Table 1. The monthly rainfall, groundwater level changes, temperature and watershed output discharge time series used in this study for 1997–1998 to 2013–2014 (204 months) are presented in Figures 5–7.

It is worth noting that the aquifer of Silakhor plain is a semi-confined aquifer surrounded by an aquitard. There are 11 different regions in this plain. Each region includes one piezometer measuring the piezometric level of the groundwater (Figure 8). As a result, the groundwater level changes time series of Silakhor plain is calculated from the average of the water level in these piezometers.

RESULTS AND DISCUSSION

The groundwater level time series analysis

As can be seen in Figure 5, the mean groundwater level of Silakhor plain was approximately 1,500.64 m in 1997 and

by 2014, it was approximately 1,497.63 m. It is obvious that in recent years, the mean groundwater level of this plain faced an unprecedented decrease of about 3 m due to human activities and climate change impacts. The signal fluctuations of the hydrological process are highly non-stationary and operate under a large range of scales varying from one day to several decades; therefore, eliciting information from the groundwater level fluctuations based on just investigating the initial, final and mean values of the groundwater level time series does not make any sense in reality. Therefore, the objective of the present paper is to investigate concepts and measures to achieve a clear and true interpretation regarding the groundwater level and other hydrologic time series. As mentioned before, wavelet transform provides useful decompositions of main time series. The wavelet-based decomposition of non-stationary time series into different scales provides an interpretation of series structure and extracts considerable knowledge about its history in time and frequency domains (Rajaei *et al.* 2010; Nourani *et al.* 2012). To accomplish this aim, the mean groundwater level time series are divided into 68-month three sub-series and each time sub-series is decomposed to multiple frequent time series by the db2 mother wavelet with decomposition levels 1 to 5. It is worth noting that after decomposition level of 5, the normalized energies (i.e. ρ_m) tend to 1 and as a result, the expressions of $Ln[\rho_m]$ become zero. Meanwhile, as illustrated in Figure 9 the reason for using the db2 wavelet function is the comparative similarity between this wavelet function signal shape and the fluctuations of the rainfall and discharge time series compared to Haar, Coif1 and Sym3 wavelet functions (Figure 3). Figure 9 shows the random part of the fluctuations in these time series.

To analyze the complexity of groundwater level time series, wavelet-entropy measure is employed. In this way, the normalized energy (ρ_n) was calculated for each decomposed time series (levels 1 to 5). Finally, a wavelet-entropy measure was obtained for each three sub-series using MATLAB programming. The results are presented in Table 2. Figure 10 illustrates the wavelet-entropy measure changes in three 68-month periods.

As illustrated in Table 2, wavelet-entropy measure faces a reduction of about 11/73% in the third time period. The decrease in wavelet-entropy measure in a period of time is

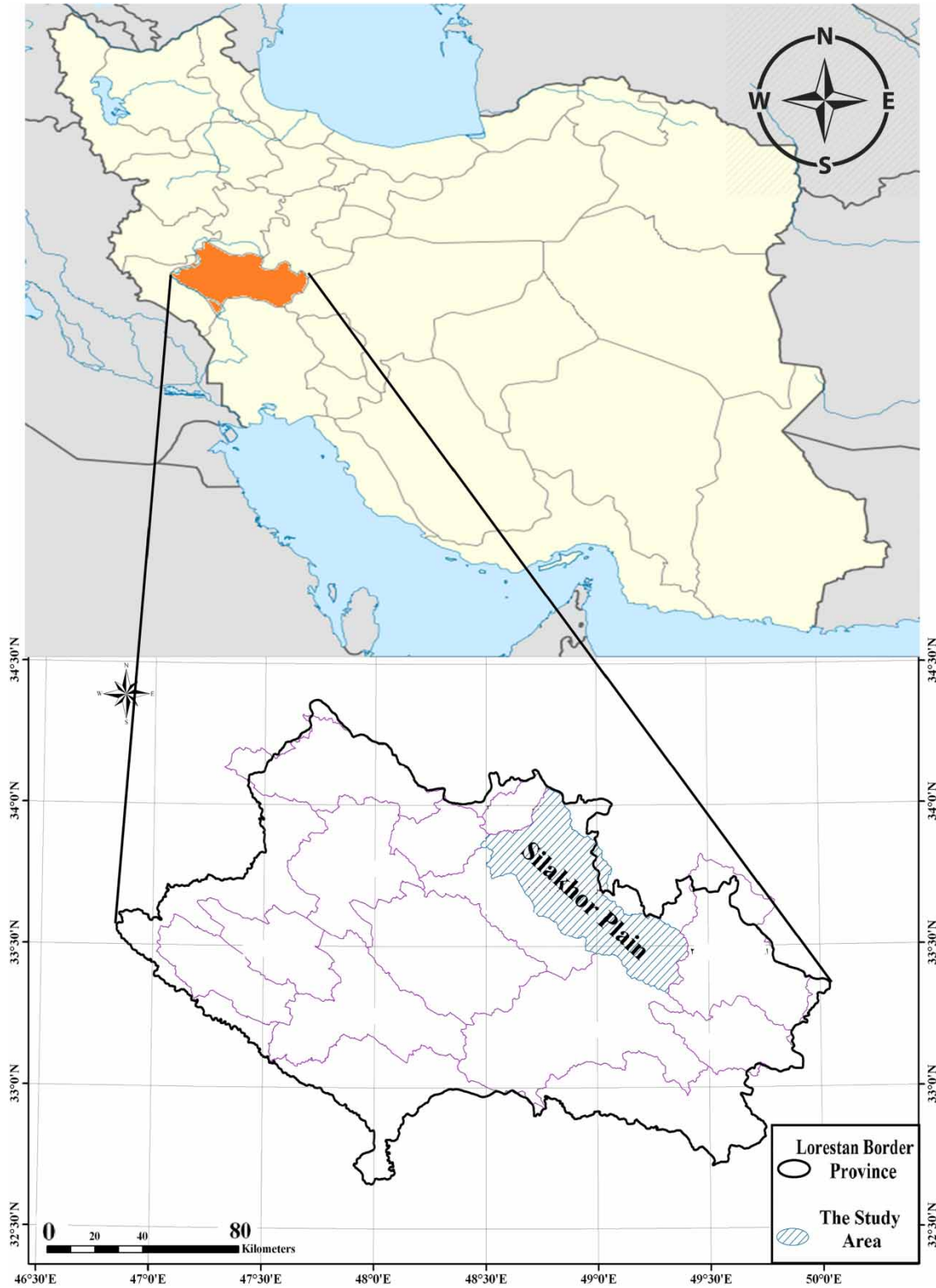


Figure 4 | Silakhor plain (location and borders).

Table 1 | Statistical characteristics for case study

Monthly time series	Max	Min	Mean	Variance
Mean groundwater level (m)	1503.2	1496.3	1499.7	5995
Rainfall (mm)	255.2	0	42.8	184
Temperature (°C)	29.9	-6	15.1	63
Output discharge (m ³ /s)	482.2	6.4	57.4	249

considered as an unfavorable trend in time series. On the other hand, the aforementioned reduction indicates the complexity decrease or the decrease in fluctuations time series of the third time period. As a result, unfavorable

trends have accrued in the groundwater level of Silakhor plain and the main aim is to assess the causes of this unfavorable event through human activities and climate change factors. It is noteworthy that the normalized energy in the decomposition level 5 is increasing suddenly for each sub-series.

Effects of human activities and climate change factors

In recent years, different human activities such as dam constructions and agricultural irrigation, changes in cropping pattern and cropping products such as rice that were not

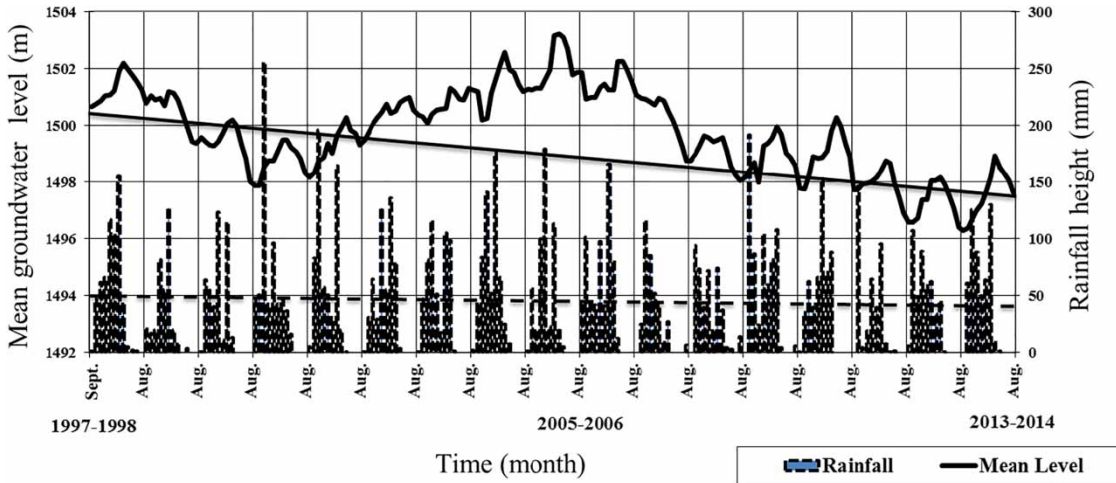


Figure 5 | Rainfall and groundwater level changes time series of Silakhor plain.

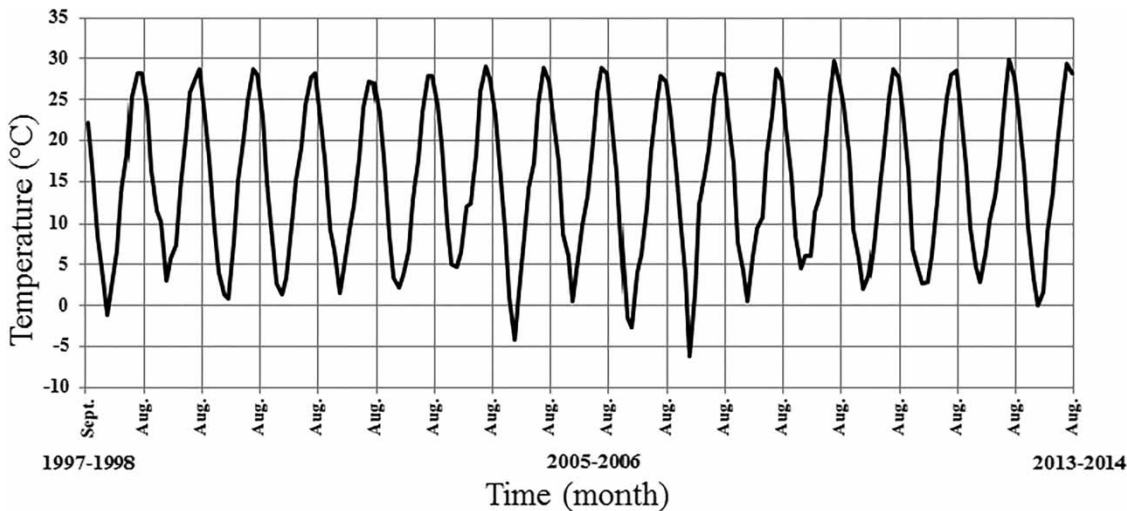


Figure 6 | Temperature time series of Silakhor plain.

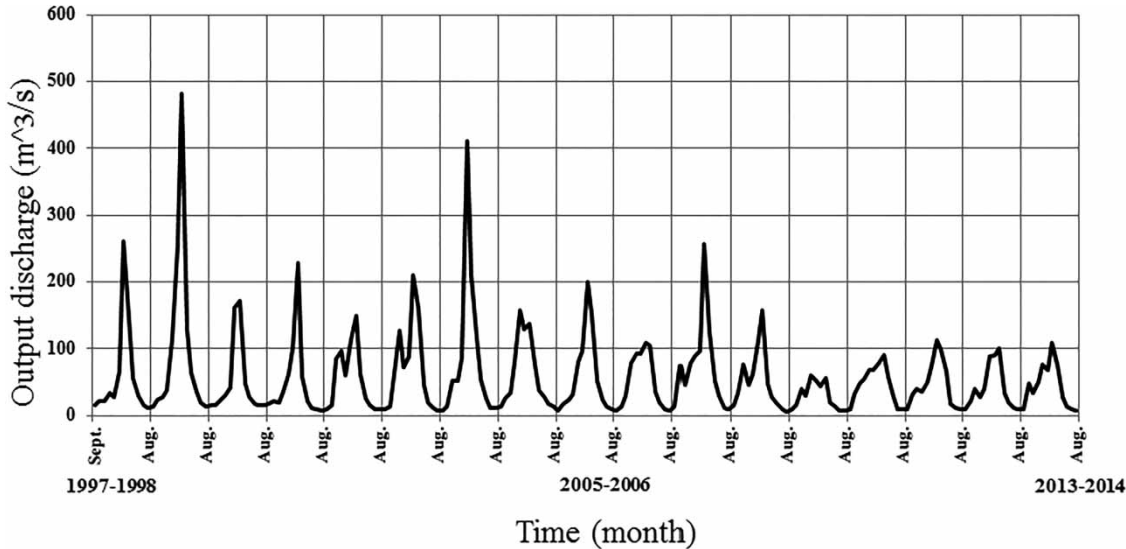


Figure 7 | Output discharge time series of Silakhor plain.

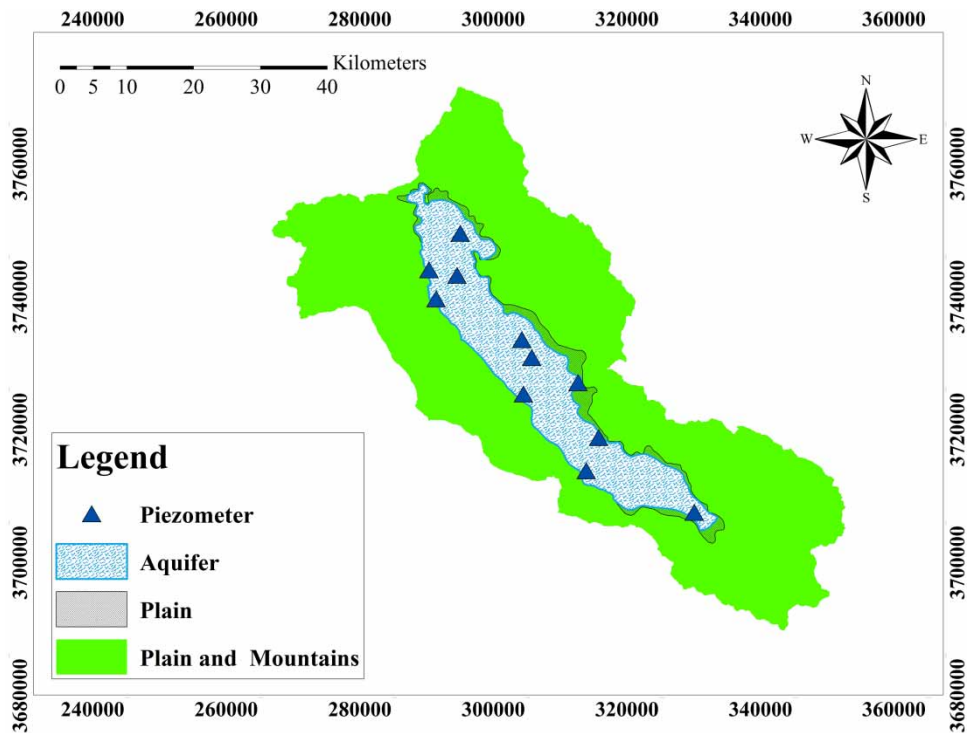


Figure 8 | The GIS map of piezometers in Silakhor plain.

compatible with the regional climate conditions, have led to high water requirements. As a result, over-exploitation of groundwater and surface water has resulted in the groundwater level reduction of Silakhor plain directly and

indirectly, respectively. Figure 11 illustrates the high density of drilled wells in this plain. According to this GIS map, 1679 wells have been drilled in Silakhor plain. As a result, the aquifer is excessively being mined, which directly

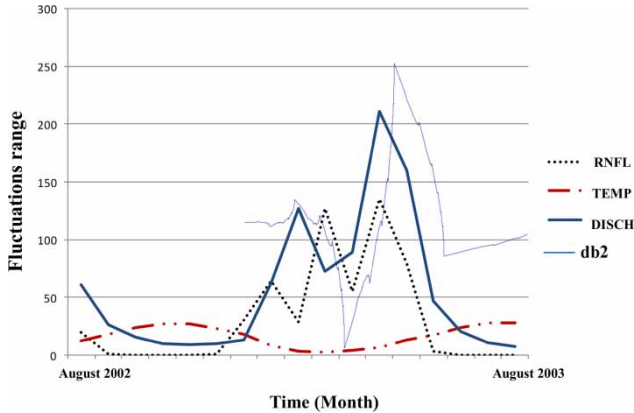


Figure 9 | The comparison between db2 wavelet function and rainfall, temperature and discharge time series.

Table 2 | Wavelet-entropy measure calculation for groundwater level time series

Normalized energy of decomposed time series	68-month three sub-series		
	First sub-series	Second sub-series	Third sub-series
ρ_1	0.000125	0.000319	0.000217
ρ_2	0.000722	0.002441	0.001165
ρ_3	0.003428	0.008336	0.009348
ρ_4	0.003751	0.010765	0.009489
ρ_5	0.99197	0.97814	0.97978
Wavelet-entropy measure (WE)	0.09983	0.12756	0.11259
Percentage changes	–	27.77%	–11.73%

Note: The wavelet-entropy measure is a dimensionless parameter.

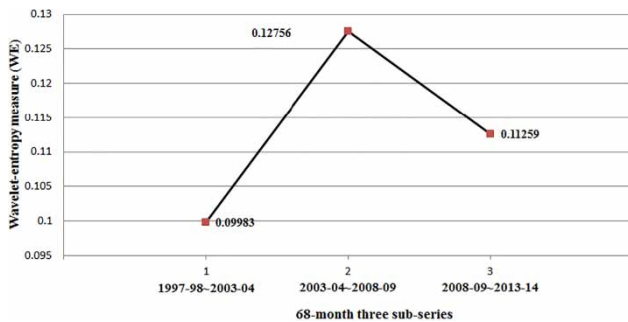


Figure 10 | Wavelet-entropy measure changes in three different periods for groundwater level time series.

contributes to the water level decline. It is obvious that groundwater exploitation plays a direct role in the decline of groundwater level.

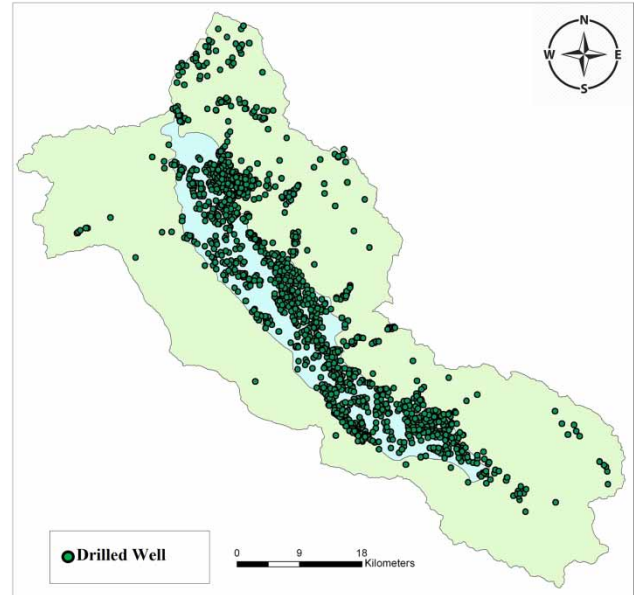


Figure 11 | Location of drilled wells in Silakhor plain.

This section aims to classify human and climatic reasons that have indirectly affected the declining groundwater level. As mentioned above, different human activities result in the output discharge flow reduction of Silakhor plain. To accomplish this aim, output discharge time series representing human activities factors (Nourani *et al.* 2015a, 2015b) and rainfall and temperature time series of Silakhor plain representing climate change factors (Nourani *et al.* 2015a, 2015b) are divided into three 68-month sub-series and each time sub-series was decomposed to multiple frequent time series by the db2 mother wavelet with decomposition levels 1 to 5 as in the previous section. Finally, wavelet-entropy measure was calculated for three sub-series of rainfall, temperature and output discharge signals. The results are presented in Tables 3–5. Figure 12 exhibits the wavelet-entropy measure changes in three 68-month periods for rainfall, temperature and output discharge signals.

As mentioned above under ‘Wavelet-entropy measure’, to decompose each sub-series, the db2 mother wavelet was used due to its resemblance to the signal fluctuations of the hydrological processes such as rainfall, temperature and output discharge time series. It appears from Table 3 that the wavelet-entropy measure for the plain rainfall time series has a reduction of about 13% in the third time period. Hence, a 13% reduction of fluctuations occurred in

Table 3 | Wavelet-entropy measure calculation for rainfall time series

Normalized energy of decomposed time series	68-month three sub-series		
	First sub-series	Second sub-series	Third sub-series
ρ_1	0.023803	0.024031	0.01974
ρ_2	0.013089	0.045677	0.036965
ρ_3	0.056131	0.098165	0.072813
ρ_4	0.015506	0.028087	0.028483
ρ_5	0.89147	0.80404	0.842
Wavelet-entropy measure (WE)	0.47441	0.73412	0.6363
Percentage changes	–	55%	–13%

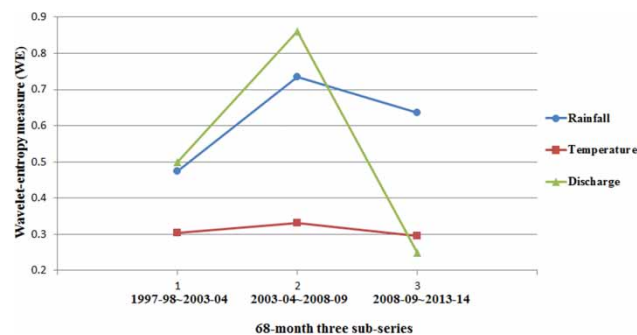
Table 4 | Wavelet-entropy measure calculation for temperature time series

Normalized energy of decomposed time series	68-month three sub-series		
	First sub-series	Second sub-series	Third sub-series
ρ_1	0.000497	0.000762	0.000419
ρ_2	0.006138	0.00628	0.006006
ρ_3	0.05269	0.039564	0.038022
ρ_4	0.010216	0.02633	0.019382
ρ_5	0.93046	0.92706	0.93617
Wavelet-entropy measure (WE)	0.30402	0.33107	0.29648
Percentage changes	–	9%	–10.5%

Table 5 | Wavelet-entropy measure calculation for output discharge time series

Normalized energy of decomposed time series	68-month three sub-series		
	First sub-series	Second sub-series	Third sub-series
ρ_1	0.014705	0.013552	0.002705
ρ_2	0.022404	0.04281	0.011389
ρ_3	0.044648	0.10664	0.015655
ρ_4	0.012512	0.087381	0.017352
ρ_5	0.90573	0.74962	0.9529
Wavelet-entropy measure (WE)	0.49946	0.8609	0.24836
Percentage changes	–	72%	–71%

the third time period of the rainfall time series. Also, Table 4 indicates that due to the slight changes of the wavelet-entropy measure for the temperature time series (9%

**Figure 12** | Wavelet-entropy measure changes in three different periods of rainfall, temperature and output discharge time series.

increase and 10.5% decrease in the second and third time period respectively), it may not have a significant impact on the groundwater declining as compared to other factors. Data from Tables 3 and 4 can be compared with the data in Table 5 which shows the remarkable reduction (71%) in the wavelet-entropy measure in the third time period of output discharge time series as compared to rainfall and temperature time series. Figure 12 provides a better understanding of wavelet-entropy changes in the current time series.

The differences between wavelet-entropy measure reductions in the third time period are highlighted in Figure 12. According to this figure, the wavelet-entropy measure reduction, which indicates the reduction of fluctuations or complexity for the output discharge time series of Silakhor plain, is much more than the other time hydrological series in the third time period (since 2008–2014). As shown in Figure 10, in this period of time, an unfavorable trend occurred in the groundwater level due to the decreased complexity. Therefore, with respect to the significant decrease in wavelet-entropy measure for output discharge in the third time period, runoff discharge changes and therefore water penetration changes could be considered as the dominant reason for the groundwater elevation decrease in Silakhor plain aquifer. On the other hand, human activities (e.g. dam constructions and agricultural irrigation, changes in cropping pattern, industrial development, indiscriminate digging of wells, etc.) play a more striking role in output discharge manipulation than the climate change factors such as rainfall and temperature changes. Another proof of this claim is the absence of significant changes in the average rainfall of this plain according to the dotted line in Figure 5.

CONCLUSIONS

Groundwater level reduction due to lack of water resources management is considered as a serious threat to human society and the environment. As a result, detecting the most dominant reasons in exacerbating the effects of groundwater level reduction needs to be addressed urgently. In this study, a multi-scale wavelet-entropy method is applied to groundwater level, rainfall, temperature and output discharge time series of Silakhor plain in order to detect the relationship between groundwater level decline and human and climatic changes. In this case, output discharge represents the factor of human activities and rainfall and temperature represent the factors of climate changes. In this way, these time series of Silakhor plain are divided into three 68-month sub-series and each time sub-series was decomposed to multiple frequent time series by the db2 mother wavelet with decomposition levels 1 to 5. Finally, wavelet-entropy measure was calculated for each sub-series. The results show that the wavelet-entropy measure for mean groundwater level time series faces a reduction in the third time period and this event is the sign of the occurrence of an unfavorable event in the groundwater time series. In this period of time, the wavelet-entropy measure for rainfall, temperature and output discharge time series faces a decrease but the major finding was that the wavelet-entropy reduction for output discharge time series is more significant than the other time series in the third time period (since 2008–2014). As a result, the most striking observation to emerge from the data comparison was the preference of the human activities factors as compared to the climate change factors in the groundwater level decline of Silakhor plain.

ACKNOWLEDGEMENTS

This research was supported by Ayatollah Boroujerdi University research center (Project number 160529-15664).

REFERENCES

Amaranto, A., Munoz-Arriola, F., Corzo, G., Solomatine, D. P. & Meyer, G. 2018 [Semi-seasonal groundwater forecast using](#)

- [multiple data-driven models in an irrigated cropland](#). *J. Hydroinform.* **20** (6), 1227–1246.
- Bercher, J. F. & Vignat, C. 2000 [Estimating the entropy of a signal with applications](#). *IEEE Signal Process. Soc.* **48** (6), 1687–1694.
- Castillo, A., Castelli, F. & Entekhabi, D. 2015 [An entropy-based measure of hydrologic complexity and its applications](#). *Water Resour. Res.* **51** (7), 5145–5160.
- Chen, J. & Li, G. 2014 [Tsallis wavelet entropy and its application in power signal analysis](#). *Entropy* **16** (6), 3009–3025.
- Chinnasamy, P. & Ganapathy, R. 2018 [Long-term variations in water storage in Peninsular Malaysia](#). *J. Hydroinform.* **20** (5), 1180–1190.
- Cimen, M. & Kisi, O. 2009 [Comparison of two different data-driven techniques in modeling lake level fluctuations in Turkey](#). *J. Hydrol.* **378** (3), 253–262.
- Costa, M., Goldberger, A. L. & Peng, C. K. 2002 [Multi-scale entropy analysis of complex physiologic time series](#). *Am. Phys. Soc.* **89** (6), 1–4.
- Deng, X., Li, F., Zhao, Y. & Li, S. 2018 [Regulation of deep groundwater based on MODFLOW in the water intake area of the south-to-north water transfer project in Tianjin](#). *China J. Hydroinform.* **20** (4), 989–1007.
- Faskhodi, A. & Mirzaie, M. 2013 [Consequences of Zayandehrood drying crisis in rural areas \(case study: Isfahan plain\)](#). *J. Rural Dev.* **5** (2), 157–180.
- Fathian, F., Modarres, R. & Dehghan, Z. 2016 [Urmia Lake water-level change detection and modeling](#). *Model. Earth Syst. Environ.* **2** (4), 203–219.
- Goupillaud, P., Grossmann, A. & Morlet, J. 1984 [Cycle-octave and related transforms in seismic signal analysis](#). *Geoexploration* **23**, 85–102.
- Hao, X., Chen, Y., Xu, C. & Li, W. 2008 [Impacts of climate change and human activities on the surface runoff in the Tarim river basin over the last fifty years](#). *Water Resour. Manage.* **22**, 1159–1171.
- Kakahaji, H., Banadaki, H. D., Kakahaji, A. & Kakahaji, A. 2013 [Prediction of Urmia Lake water-level fluctuations by using analytical, linear statistic and intelligent methods](#). *Water Resour. Manage.* **27** (13), 4469–4492.
- Kebede, S., Travi, Y., Alemayehu, T. & Marc, V. 2006 [Water balance of Lake Tana and its sensitivity to fluctuations in rainfall, Blue Nile basin, Ethiopia](#). *J. Hydrol.* **316** (1–4), 233–247.
- Komasi, M. & Sharghi, S. 2016 [Hybrid wavelet-support vector machine approach for modelling rainfall-runoff process](#). *Water Sci. Technol.* **73** (8), 1937–1953.
- Labat, D. 2005 [Recent advances in wavelet analyses: Part 1. A review of concepts](#). *J. Hydrol.* **314** (1–4), 275–288.
- Mallat, S. G. 1998 *A Wavelet Tour of Signal Processing*, 2nd edn. Academic Press, San Diego.
- Ming Chou, C. 2011 [Wavelet-based multi-scale entropy analysis of complex rainfall time series](#). *Entropy* **13** (1), 241–253.
- Mishra, A. K., Özger, M. & Singh, V. P. 2009 [An entropy-based investigation into the variability of rainfall](#). *J. Hydrol.* **370** (1–4), 139–154.

- Nourani, V., Komasi, M. & Taghi Alami, M. 2012 Hybrid wavelet-genetic programming approach to optimize artificial neural network modeling of rainfall-runoff process. *J. Hydrol. Eng.* **17** (6), 724–741.
- Nourani, V., Ranjbar, S. & Tootoonchi, F. 2015a Change detection of hydrological processes using wavelet-entropy complexity measure case study: Urmia Lake. *J. Civil Environ. Eng.* **45** (3), 75–86.
- Nourani, V., Sharghi, E. & Ranjbar, S. 2015b Change detection of hydrological processes using wavelet-entropy complexity measure (case study: Urmia Lake Watershed). In: *Symposium on Regional Floods: Regional Effects of Changes in the River System*. Vienna University of Technology, Austria.
- Pincus, S. M. 1991 Approximate entropy as a measure of system complexity. *Proc. Natl. Acad. Sci. USA* **88** (6), 2297–2301.
- Rabbani, F. & Alikhani, A. 2010 Regional analysis of climate change (drought) in Karaj River catchment. In *Scientific Conference on Water Challenges in Qom*. Qom University, Iran.
- Rajaei, T., Mirbagheri, S. A., Nourani, V. & Alikhani, A. 2010 Prediction of daily suspended sediment load using wavelet and neuro-fuzzy combined model. *J. Environ. Sci. Technol.* **7** (1), 93–110.
- Richman, J. S. & Moorman, J. R. 2000 Physiological time-series analysis using approximate entropy and sample entropy. *Am. J. Physiol. Heart Circ. Physiol.* **278** (6), 2039–2049.
- Rosso, O. A. & Mairal, M. L. 2001 Characterization of time dynamical evolution of electroencephalographic records. *Physica A* **312**, 469–504.
- Rosso, O. A., Blanco, S., Yordanova, J., Kolev, V., Figliola, A. & Schurmann, M. 2001 Wavelet entropy: a new tool for the analysis of short duration brain electrical signals. *J. Neurosci. Meth.* **105**, 65–75.
- Rosso, O. A., Martin, M. T., Figliola, A., Keller, K. & Plastino, A. 2006 EEG analysis using wavelet-based information tools. *J. Neurosci. Meth.* **153**, 163–182.
- Shannon, C. E. 1948 A mathematical theory of communications I and II. *Bell. Syst. Tech.* **27** (3), 379–443.
- Shardt Yuri, A. W. & Huang, B. 2013 Statistical properties of signal entropy for use in detecting changes in time series data. *J. Chemometr.* **27** (11), 394–405.
- Singh, V. P. & Cui, H. 2015 Entropy theory for groundwater modeling. *J. Groundwater Res.* **3** (4), 1–12.
- Singh, M. K., Singh, V. P. & Das, P. 2016 Mathematical modeling for solute transport in aquifer. *J. Hydroinform.* **18** (3), 481–499.
- Vaheddoost, B. & Aksoy, H. 2017 Structural characteristics of annual precipitation in Lake Urmia basin. *Theor. Appl. Climatol.* **128** (3–4), 919–932.
- Vahidi, A. 2011 Impact of climate change and drought on water resources in Iran. In: *The Fifth Conference of Watershed Management and Soil and Water Resource Management*. The Iranian Society of Irrigation and Water, Iran.
- Varanis, M. & Pederiva, R. 2015 Wavelet packet energy-entropy feature extraction and principal component analysis for signal classification. *Proc. Brazil. Soc. Appl. Comput. Math.* **3** (1), 1–7.
- Varouchakis, E. A., Palogos, I. & Karatzas, G. P. 2016 Application of Bayesian and cost benefit risk analysis in water resources management. *J. Hydrol.* **534**, 390–396.
- Waibel, M. S., Gannett, M. W., Chang, H. & Hulbe, C. L. 2013 Spatial variability of the response to climate change in regional groundwater systems – examples from simulations in the Deschutes basin, Oregon. *J. Hydrol.* **486**, 187–201.
- Xue, L., Guomin, L. & Yuan, Z. 2014 Identifying major factors affecting groundwater change in the north China plain with grey relational analysis. *Water* **6** (6), 1581–1600.
- Yang, Q., Zhang, J., Hou, Z., Lei, X., Tai, W., Chen, W. & Chen, T. 2017 Shallow groundwater quality assessment: use of the improved Nemerow pollution index, wavelet transform and neural networks. *J. Hydroinform.* **19** (5), 784–794.
- Zwolsman, J. J. G. & van Bokhoven, A. J. 2007 Impact of summer droughts on water quality of the Rhine River – a preview of climate change. *Water Sci. Technol.* **56** (4), 45–55.

First received 9 October 2018; accepted in revised form 27 January 2019. Available online 8 March 2019